

The First Full-Scale Prototype of a BIL MDT Chamber for the ATLAS Muon Spectrometer

A. Biscossa, M. Cambiaghi, C. Conta, R. Ferrari, M. Fraternali, A. Freddi, G. Iuvino,
A. Lanza, M. Livan, A. Negri, G. Polesello, A. Rimoldi, V. Vercesi, F. Vercellati
(University of Pavia and INFN)

P. Bagnaia, C. Bini, G. Capradossi, G. Ciapetti, G. De Zorzi, M. Iannone, F. Lacava,
A. Mattei, L. Nisati, P. Oberson, L. Pontecorvo, S. Rosati, S. Veneziano, A. Zullo
(University of Rome and INFN)

C. Daly, R. Davisson, H. Guldenmann, H. Lubatti, T. Zhao
(University of Washington, Seattle)

1.0 Introduction

In this note we describe the construction of the first full-scale prototype of a BIL MDT chamber for the barrel part of the ATLAS muon spectrometer. Our goal was to test the assembly structure and assembly procedures. In addition, tube construction, end-plug and wire locator design and the on-chamber gas distribution system have been tested.

The chamber design followed the concept developed by the ATLAS Muon Working Group and described in the ATLAS Technical Proposal [1]. Two multilayers, consisting of 3 layers of 30 mm diameter aluminium tubes, are glued to the two sides of a very light spacer/support structure with 150 mm separation between the two multilayers. Each multilayer contains a total of 96 drift tubes, 2.6 m long. In this way each charged track crossing the chamber will be accurately measured both in position and direction.

Design specifications aim for 20 μm accuracy (σ) in the location of each wire at the ends of the drift tube where the wire is fixed and a wire-tube concentricity better than 100 μm (tolerance) elsewhere. In the following, the chamber construction procedure and the end-plug/wire locator design are described in detail. Tests of the chamber structure under static and thermal loads are also presented. We conclude with preliminary results on the chamber performance at the H8 CERN test beam.

2.0 The assembly structure and the construction procedure

The basic concept of the jigging structure has been developed starting from the original proposal of the Seattle group for the trapezoidal end-cap chambers [2]. For barrel chambers there are simplifications because of the rectangular chamber shape and the smaller dimensions.

The assembly jigging is supported on a 1.5 × 3.0 m marble table which has very good planarity ($\pm 4 \mu\text{m}$ tolerance on the whole surface). High precision pairs of combs (bottom comb, top comb) are used to control the position of the individual tubes in the top and bottom layers. In all, seven pairs of combs (1.2 m long) have been used. These are equally spaced (~ 0.43 m) over the 2.56 m active length of the tubes.

Combs are machined in pairs by boring 40 cylindrical grooves, 30.010 mm diameter, with a pitch of 30.010 mm, on the top of the combs. The grooves in the jig combs were created by a simple boring operation and are thus shaped as a part of a circle. This has several advantages:

1. This is the most accurate and least expensive way to make the grooves.
2. A round groove will locate a tube more accurately than a V-groove. It is not possible to choose an optimum V-groove angle as the tubes do not have a predictable out of round shape and this shape varies along the length of the tube.
3. Away from the end plugs, the tubes are out of round in some random way. Round grooves will tend to deform the tubes into a more round shape. V-grooves do the opposite.

Round grooves have more surface area to which foreign matter can adhere. Grooves of any shape require inspection and cleaning each time just before a layer of tubes is loaded into the jig.

At the end plugs the tube is both forced to be round and is made rigid. This implies that we cannot tolerate any oversize tubes. Oversize in this case means that the tube outer diameter is greater than the pitch built into the jigging. In the BIL jigging this condition is met by using a jig pitch of 30.010 mm and by checking each tube with a GO/NOGO gauge to ensure that any tubes which exceed the manufactured tolerance of 30.000 mm are rejected¹. The nominal minimum clearance of 10 μm was used to be conservative on this first prototype and can be reduced to 5 or even 0 μm . Also, as the tubes are very round at the end plugs, the middle layer is located accurately by the two other layers which are located precisely by the jigging.

Elsewhere along the tubes, the tubes are supported at about 0.43 m intervals by jigging combs. Here the tubes are not solid in cross section and are not so round. At the combs, the top and bottom layers are held accurately. This leaves unsupported spaces between the jig combs. With a 0.43 m space, gravitational deflection of a single tube is negligible. Applying glue after stacking avoids tube deflection due to squeezing the glue out of the places where the tubes touch. This leaves the straightness of the tubes as the only source of error. If the tubes are nominally touching or have an average gap

1. Note that experience with electromagnetic crimping of the end plugs has shown that there is no increase in tube diameter at the crimp.

of 10 μm or less, then an out of straight tube may touch its neighbours. If, for example, the out of straightness is 100 μm or more, several neighbouring tubes will now touch. However, if these tubes are to be deflected, they will push back on the offending tube, thus limiting its out of straightness. There is certainly no long distance propagation and, as the out of straightness of the tubes is random in direction, these effects will average out in an assembly of tubes. In short, with touching tubes, these effects are self correcting. However, if a 100 μm gap is left between the tubes, any tube can get to the tolerance limit without any control from its neighbours. If it is over 100 μm out of straight, there will not be enough correcting force to put it back in tolerance. The gap simply allows tubes to be out of tolerance.

In the same machining set-up two additional grooves are bored on the opposite side of the bottom combs (see fig. 2.1 and 2.2). These are used to locate the combs on the marble table with two stainless steel high-precision rods that position on these grooves. In this way the planarity of the tube locating grooves is established by the marble table. The height of the combs was chosen so as to limit the deflection of any

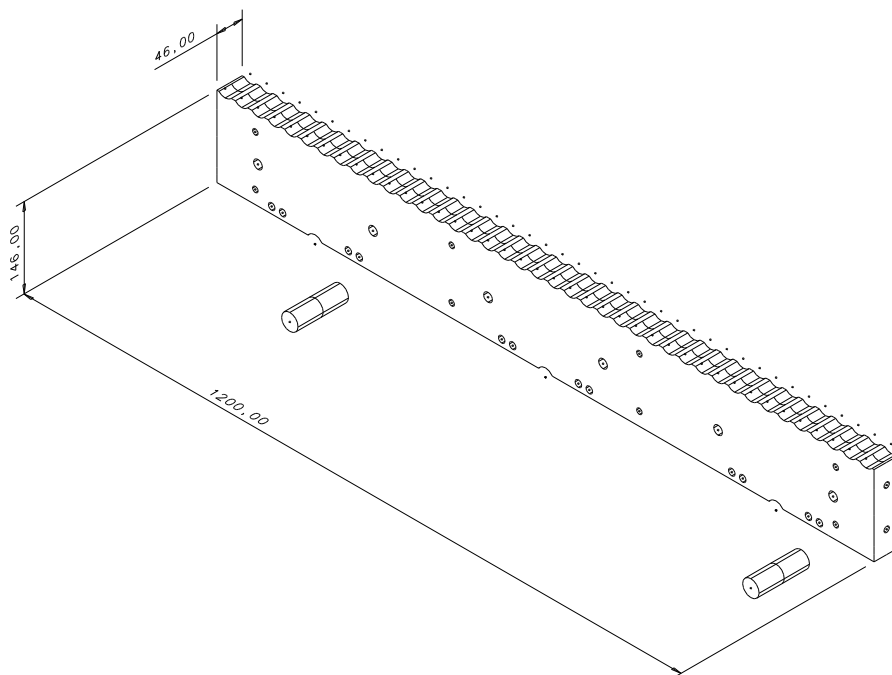


Figure 2.1 Bottom comb

comb to less than 5 μm normal to the table

After machining each comb was measured using a coordinate measuring machine ($\sigma \sim 2 \mu\text{m}$). The axis of each of the 40 grooves was reconstructed from 9 measured points on each groove. Table 2.1 summarizes the result on the pitch and the height. As can be seen an average pitch of 30.009 mm, $\sigma_{\text{pitch}} \sim 4 \mu\text{m}$, and $\sigma_z \sim 5 \mu\text{m}$ has been achieved. The two best combs (# 1, 7) were used for the two extreme positions of the assembly structure to obtain the best possible positioning at the wire locators.

The seven combs, each sitting on the two precision rods, were then placed on the marble table and tied together by precisely machined tiles (see fig. 2.3). The tiles have

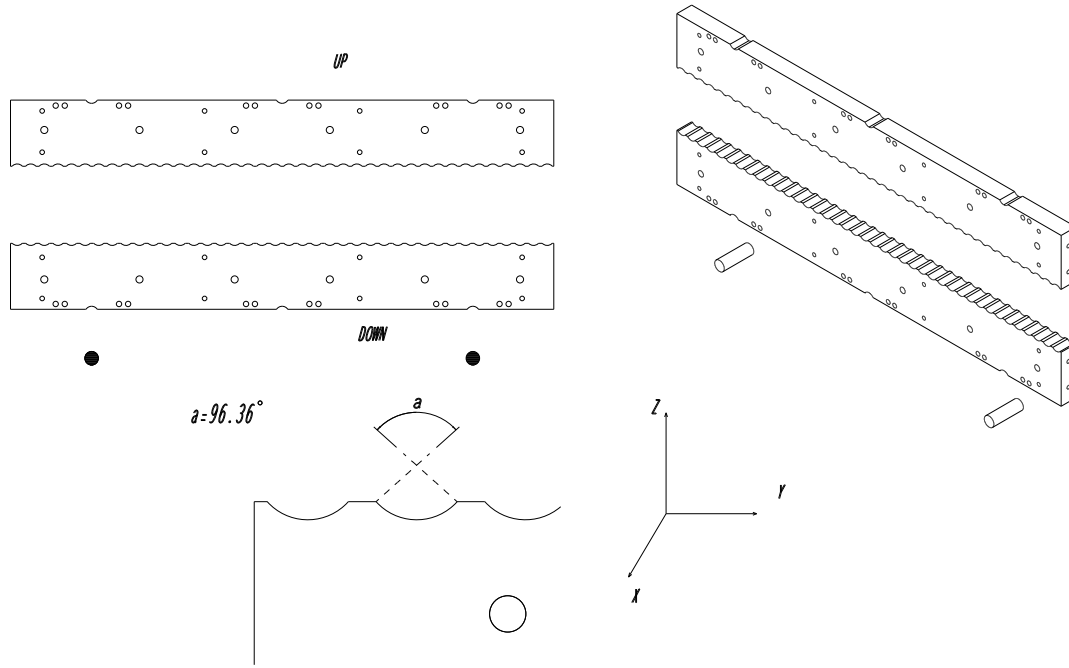


Figure 2.2 Top and bottom combs

Table 2.1 Results on pitch measurements

Comb #	Average pitch (mm)	σ_{pitch} (μm)	σ_z (μm)
1	30.010	3	4
2	30.008	4	5
3	30.008	3	6
4	30.007	3	3
5	30.009	6	6
6	30.010	3	5
7	30.009	4	3

a $\pm 5 \mu\text{m}$ tolerance at the contact surfaces. The function of the tiles is to guarantee the parallelism of the combs in the horizontal and vertical planes. The width of the tiles is matched to the distance between the two internal wire locators; in this way the locators which define the wire position are sitting at the external edges of the two extreme combs. After assembly, the height of the grooves with respect to the reference table for the first and last comb was measured and a maximum of $6 \mu\text{m}$ deviation from planarity was observed. The relative alignment of the groove axis for all the combs was obtained using a thin wire stretched between two external supports (see fig. 2.3 and ref. 3); the accuracy achieved was at the level of $10 \mu\text{m}$.

Multilayer assembly proceeded by positioning three layers of 32 tubes each on the bottom jig between two side walls. The side walls are made by bonding precision rods together (see fig. 2.5). The diameter of the rods (2.9985 cm) was selected to match the

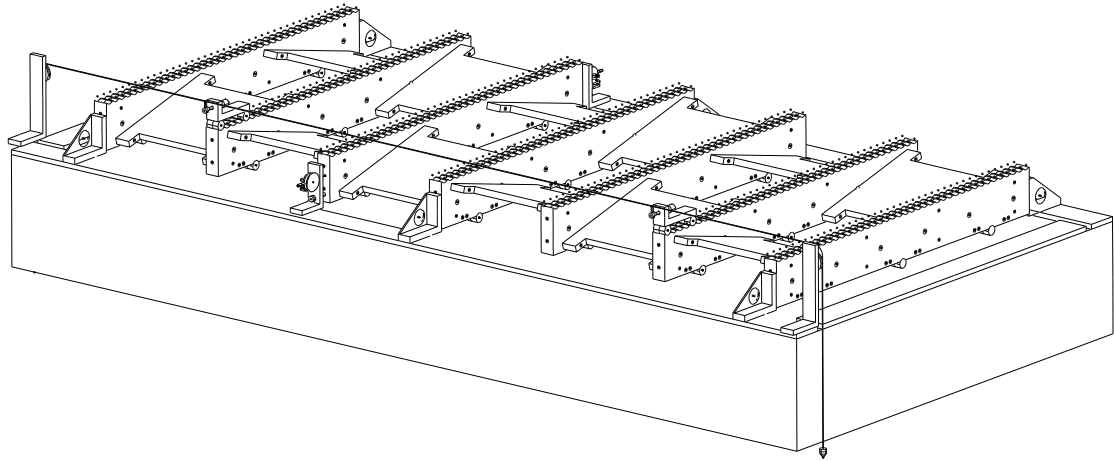


Figure 2.3 Bottom combs on granite table showing alignment wire

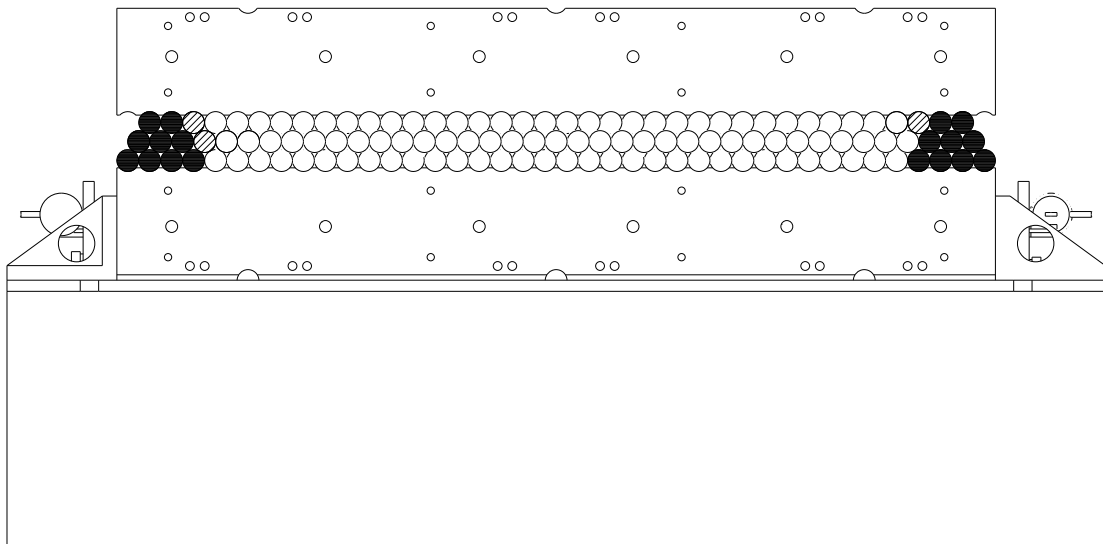


Figure 2.4 View of multilayer in assembly jig showing side walls

average diameter of the tubes. Additional dummy tubes (see fig. 2.4 - dashed tubes) are used to obtain the desired V-shape of the multilayer.

The seven upper combs, controlling the top layer, were then placed in position (see figs. 2.4 and 2.6). A reference plate at one end of the jig was used to fix the axial position of each tube during assembly. This plate established the planarity of the surface defined by the outside of the end plugs (needed for good gas tightness of the gas distribution jumpers, see section 6).

The gluing was performed with 3M DP460 glue injected in the three contact points between three adjacent tubes using the nozzle developed in Seattle [4] (see fig. 2.7). The nozzle is inserted in the inter-tube holes and the epoxy pumped by a pneumatic gun. The nozzle extraction speed (3 cm/s) was adjusted for a glue deposition of $120 \text{ mm}^3/\text{s}$, corresponding to a glued section $\sim 4 \text{ mm}$ wide (see fig. 2.8). A total of

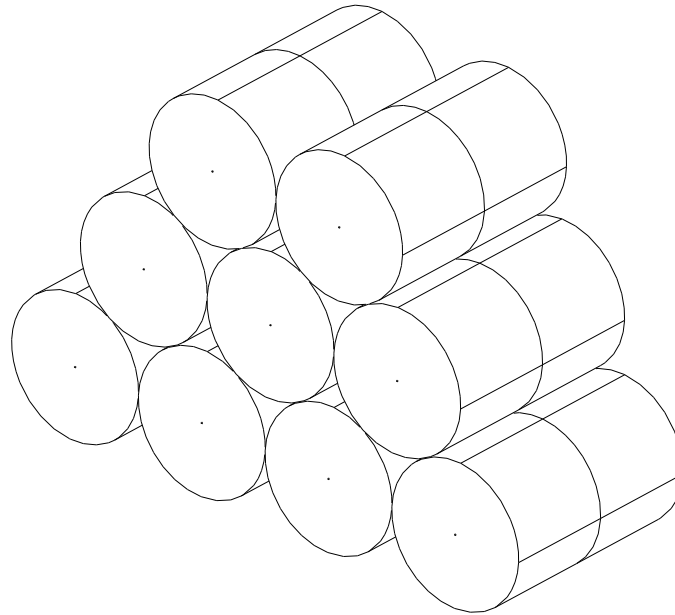


Figure 2.5 Side wall constructed from precision rods

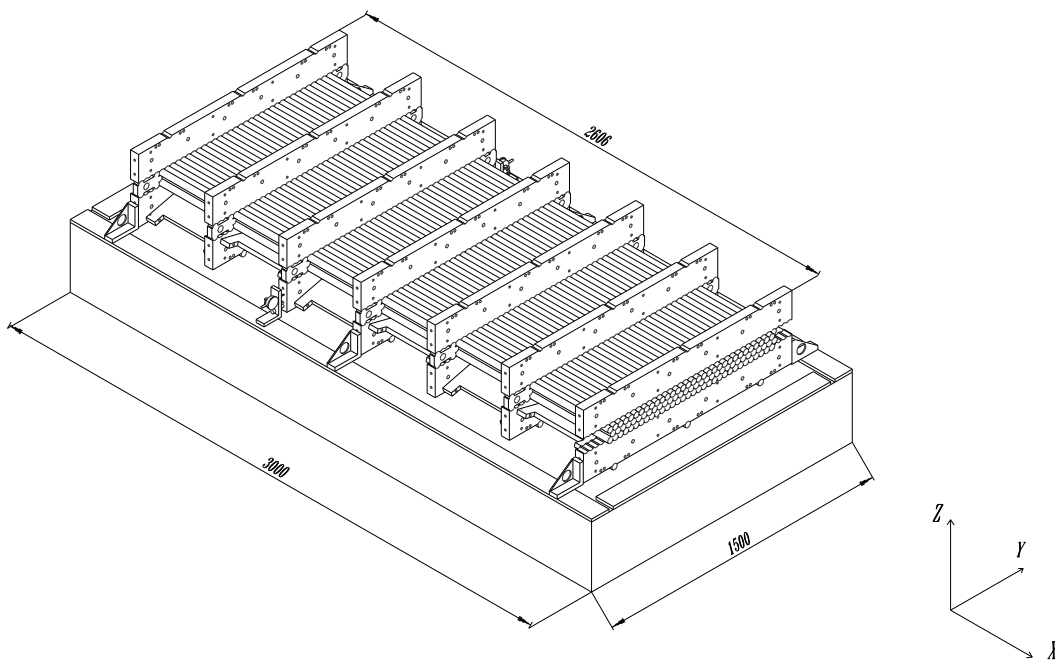


Figure 2.6 Multilayer in assembly jig

$\sim 1200 \text{ cm}^3$ of glue was used per multilayer, and the total time used for glue deposition was $\sim 160 \text{ min}$ (a multi-nozzle system can easily reduce the gluing time below 1 h).

Aluminium shear plates, 1 mm thick, 100 mm wide, were glued 3-4 hours later to the top and bottom surface of the multilayer in the free space between the combs. This improves the rigidity of the structure.

After the epoxy was allowed to cure for 24 hours, the top combs were removed. Pairs of support jig blocks (see fig. 2.9) were attached to the ends of each of the three

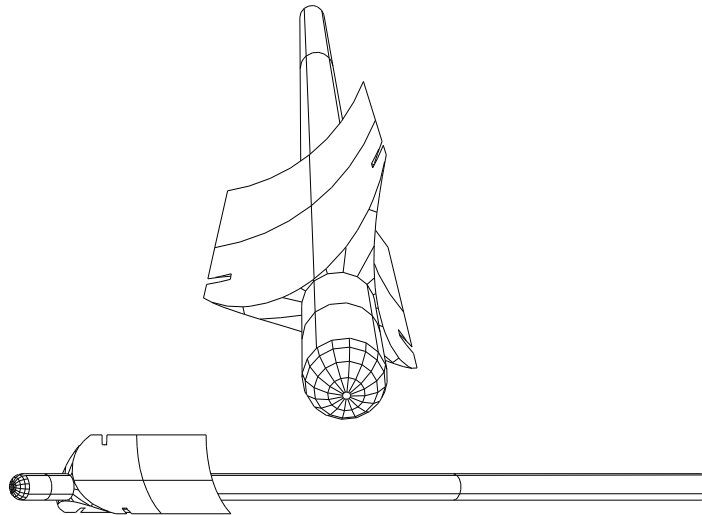


Figure 2.7 Glue dispenser head

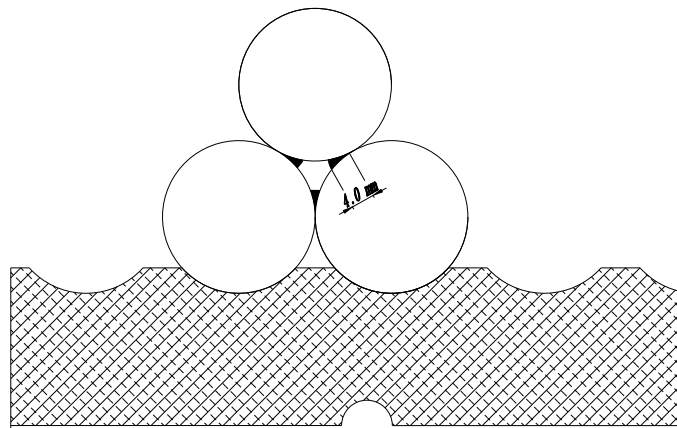


Figure 2.8 Example of glue beads

cross plates and these assemblies were placed in position on the side walls. The cross plates were held above the multilayer with a gap of 0.5 mm. This allowed room for the DP490¹ epoxy which glues the cross plates to the multilayer and also obviates the need for precise machining of the cross plate. The desired precise distance between the multilayers was determined by the precision of the support jig blocks. The longitudinal beams were glued in place using large area angle brackets and DP490 epoxy. After the epoxy had cured the whole assembly of tubes, spacer/support and the support jig blocks (Fig. 2.10) was removed from the jig.

The second multilayer was then assembled in the same way as the first one and was allowed to cure. The top combs were removed and the assembly of the first multilayer and spacer was inverted and positioned above the second multilayer. The surfaces of the support jig blocks were now positioned by the side walls thus holding the first multilayer at the desired 150 mm distance from the second multilayer. Again, the

1. This type of glue was particularly suited for the filling of the gap between spacer and multilayer due to its high viscosity.



Figure 2.9 Support jig bloks

0.5 mm gap between the cross plates and the tubes was filled with DP490 epoxy. Once this had cured, the mechanical assembly was complete. The zero readings of the in-plane alignment system (see Section 4) were then established by reading out the RASNIK with the complete chamber still in the jig.

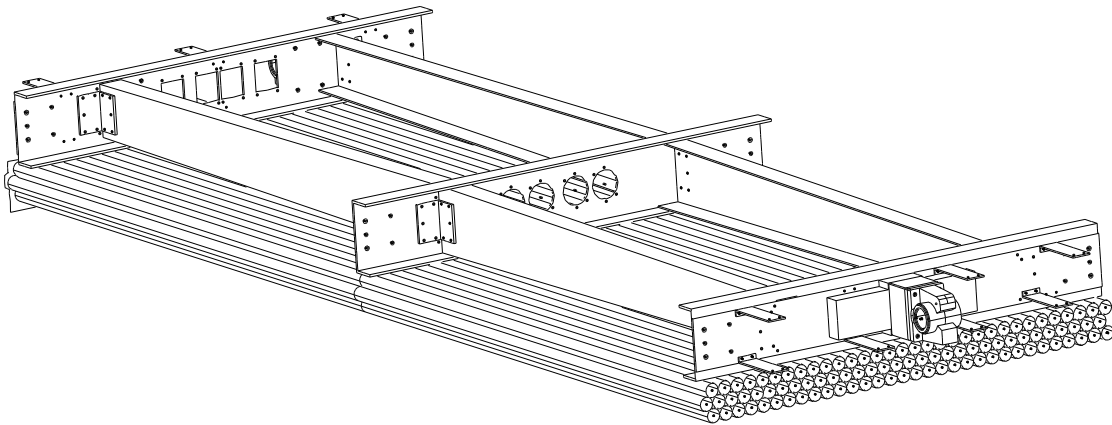


Figure 2.10 Assembly of first multilayer and spacer support structure

The assembly operation was performed at 23 C° in a clean room which was temperature controlled to $\pm 1^\circ$. The total construction time was 4 working days. Figure 2.11 shows the assembled chamber.

In order to validate the multilayer assembly method before building the full prototype, we assembled a small section of a multilayer. This was 15 tubes wide and 1.3 m long. No end plugs were used in the tubes. This resulted in reduced accuracy as the end plugs and the crimping operation do improve the roundness of the tubes. This test section was measured using a coordinate measuring machine. Eight points were measured with a resolution of $\sim 2 \mu\text{m}$ around the inner circumference of each tube at a distance of $\sim 2 \text{ mm}$ from each tube end. A circle was fitted to the set of 8 points and the position of the centre of each tube was then determined¹.

1. Final verification of the wire location accuracy is under way at the CERN X-ray tomograph. Preliminary results from one dimensional analysis, using only one X-ray beam, indicate that the standard deviation of the distances between measured wire positions and the nominal pitch is less than $20 \mu\text{m}$.

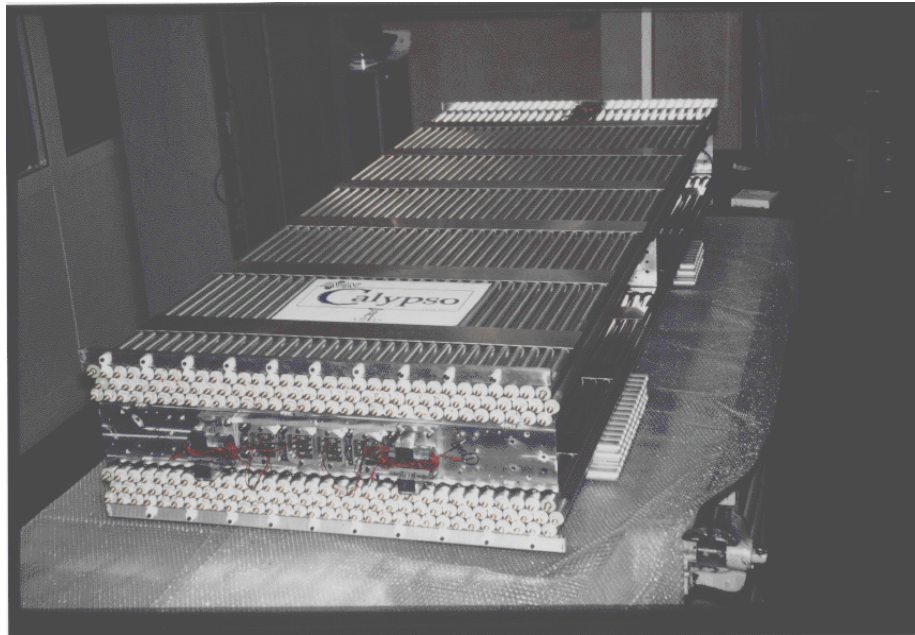


Figure 2.11 The completed BIL chamber Calypso

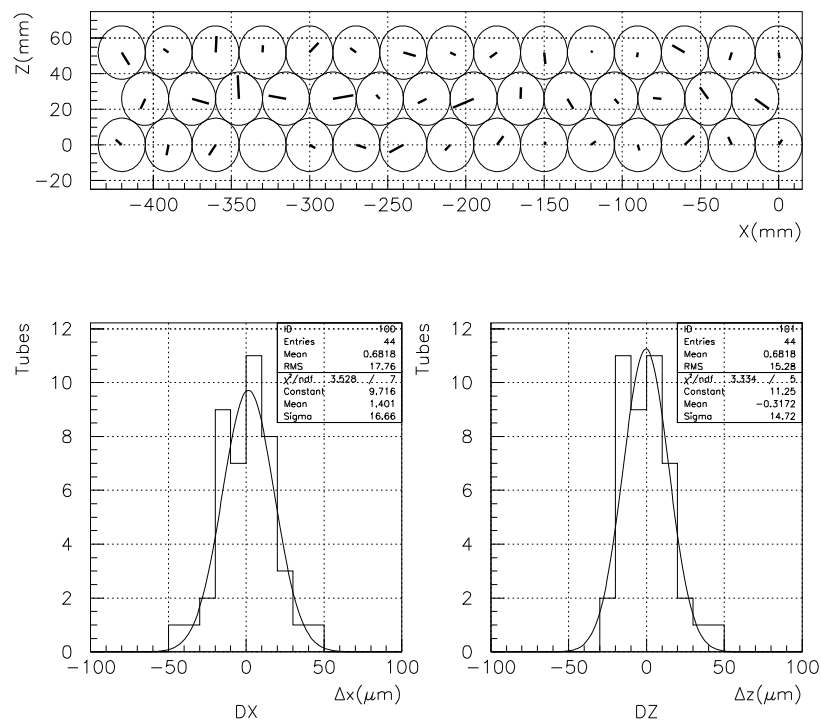


Figure 2.12 Results on measurements on 15 tube test section

The results of the comparison between the measured and nominal wire positions is shown in fig. 2.12. Segments in the upper part of the figure represent the deviations of the measured tube centre respect to the nominal positions (magnified 300 times). The errors in y (horizontal) and z (vertical) are at the level of $20 \mu\text{m}$ rms and no systematic effects are observed.

3.0 Spacer/Support Structure

The design of the spacer/support structure is based on the generic chamber design developed in Seattle for the forward region MDT chambers. The spacer/support structure is required not only to support the multilayers with the desired spacing but also to ensure that under all circumstances of use the tubes remain coaxial to the anode wires to within some allotted tolerance.

The presumed circumstances of use include, beyond mounting in some particular orientation in the ATLAS detector, an unanticipated and uncompensated thermal excursion in which the temperature of one multilayer changes by three Kelvin relative to its partner with everything else remaining isothermal. This last specification severely limits the use of the multilayers as structural elements and forces the spacer/support to take the form of a chassis upon which the multilayers are attached.

In use the essential difference between forward and barrel chambers is that the former do not have any significant out-of-plane gravitational loads and thus have no significant out of plane deflection. For the BIL chambers, there is such an out-of-plane load and it depends on the azimuthal position of a given chamber. Thus, the spacer/support structure is designed so that the natural sag of the chamber under gravity approximates the sag of the wire. An adjustable tension member allows one to fine tune the chamber sag.

The BIL chambers are quite short (~2.5 m) and have a multilayer separation of only 150 mm. This results in a different design challenge from that presented for the large barrel chambers. The challenge is to make the BIL chambers stiff enough that when mounted they deflect only by the wire sag of approximately 100 μm , use a minimum of material and still decouple the multilayers from the spacer/support in order to minimize the effects of thermal gradients.

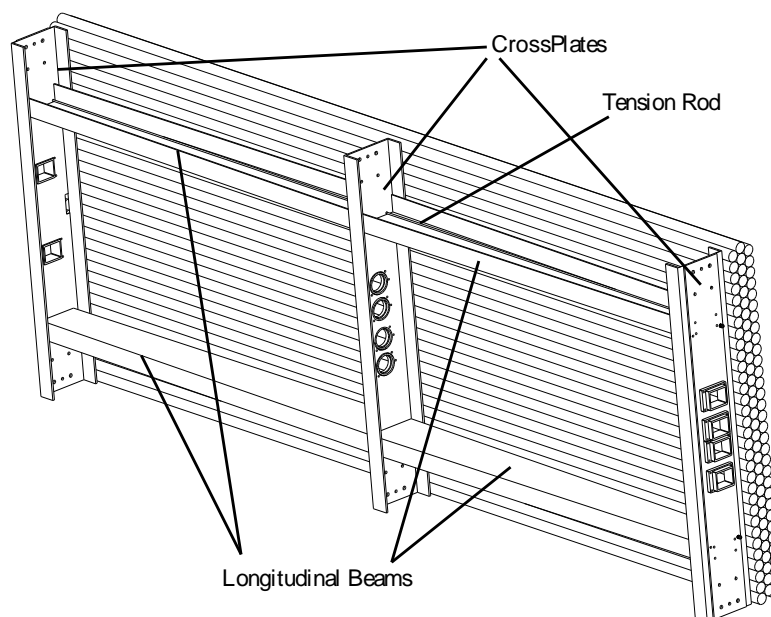


Figure 3.1 Spacer/support structure attached to one multilayer

The spacer/support structure is shown in fig. 3.1. It is comprised of three beams transverse to the tubes (cross plates) and two parallel (longitudinal beams) to the tubes all firmly joined together where they meet. The multilayers stand free from the longitudinal beams but are glued to the flanges of the cross beams.

The cross beams are in good thermal contact with the multilayers. In the circumstances of the specified thermal event there will be a temperature gradient through the depth of the cross beams and they will bow out toward the hot side. This, however, does not disturb the wire-tube concentricity since all three cross beams will deform alike merely moving tubes as a whole without distortion.

If there were truly a uniform thermal gradient through the depth of the chamber it would bow along the axis of the tubes with the same curvature that it bows across the chamber. The wires would not partake of this bending and the concentricity requirement would be violated. We do not have a uniform thermal gradient. The longitudinal beams are not in thermal contact with the multilayers and we assume that the thermal gradient through them is minuscule; therefore, the longitudinal beams on their own would remain straight. The trick then is to have the longitudinal beams control the out-of-plane position of three multilayers without having the longitudinal expansion of the tubes bend the beams. This is achieved by making the top and bottom 20 mm of the webs of the outer cross beams flexible. They are made flexible by machining them down from 6 mm to 1 mm.

The cross beams are made from 6 mm aluminium plate bent to shape and then machined as required. The height is 1 mm less than the desired separation between multilayers. This leaves space for the epoxy adhesives and eliminates the need for precise machining of this dimension. The only precision machining needed is for the dowel holes which locate the cross beams to the assembly jiggling and the mounting surfaces for the in-plane alignment system components.

The longitudinal beams which provide most of the longitudinal bending are made of 3 mm aluminium sheet bent to provide the desired section and again machined where needed. To accommodate the stiffness requirements for the BIL chamber the beam was tapered in-depth, made deepest at the middle cross beam.

Two tension rods off-centre with respect to the longitudinal beam provide for adjustment of the chamber sag to the desired value. Experience with chamber construction at NIKHEF and MPI suggests that there will always be small residual stresses after assembly and consequently the chambers will have some small, random, built-in sag. The BIL chamber design is such that its sag will always be greater than the wire sag and that the tension rods will always be able to bring the sag to the correct value.

4.0 In-plane alignment system

The measurement of the in-plane alignment of the BIL MDT prototype is provided by four RASNIK lines (fig. 4.1). The two lines on each side of the chamber, (light rays 1 and 4 on fig. 4.1) are parallel to the tubes and the two central ones (light rays 2 and 3) make an angle of ± 54 mrad with the tubes. The RASNIK elements (4 masks, 4 lenses and 2 CCD cameras) are mounted on supports that are screwed and dowelled directly on the cross-plates¹.

A lens focal length of 640 mm was chosen in order to obtain a 1 to 1 magnification at a distance of 2560 mm which is the nominal distance between the two external cross-plates. In fact, the actual lens focal length specification was $640 \text{ mm} \pm 2 \text{ mm}$. This implies a possible variation of the total length of the RASNIK lines of $\pm 8 \text{ mm}$. In order to get sharp enough pictures, each individual camera position was fine tuned using small spacers. The size of these small spacers is given in Table 4.1.

Table 4.1 RASNIK spacers size

RASNIK	Size of the small spacer
1	10 mm
2	7 mm
3	3 mm
4	5 mm

After assembly of the spacer/support, 100 pictures were taken in order to test the accuracy and stability of the RASNIK. The distribution of the reconstructed positions and rotation angles of the crossplates around the x axis are shown on Fig. 4.2. Note that the resolution in both y and z directions (i.e. perpendicular to the optical axis) is better than $0.5 \mu\text{m}$.

Tests have shown that, in order to obtain stable results for the reconstructed positions and angles, before taking the pictures it is necessary to wait at least five minutes after switching on the CCD cameras. Tests have also been made to determine the RASNIK ability to reconstruct movements in x, y and z directions. In order to do this, the RASNIK elements were mounted on an optical bench. The focal length of the lens used for these tests was 200 mm. The support of the lens contained three micrometric translators that allowed movement of the lens in y (horizontally, perpendicular to the optical axis), z (vertically) and x (horizontally, along the optical axis) directions. The range of these translators was 15 mm and their precision was $\pm 10 \mu\text{m}$. The result of the linearity tests is shown on fig. 4.2 and Table 4.2. The biggest differences between the RASNIK measurements and the mechanical translators are in the range $\pm 5 \mu\text{m}$, in good agreement with resolution of the translators.

1. Masks and cameras have been produced at NIKHEF, while the lenses have been manufactured in Protvino.

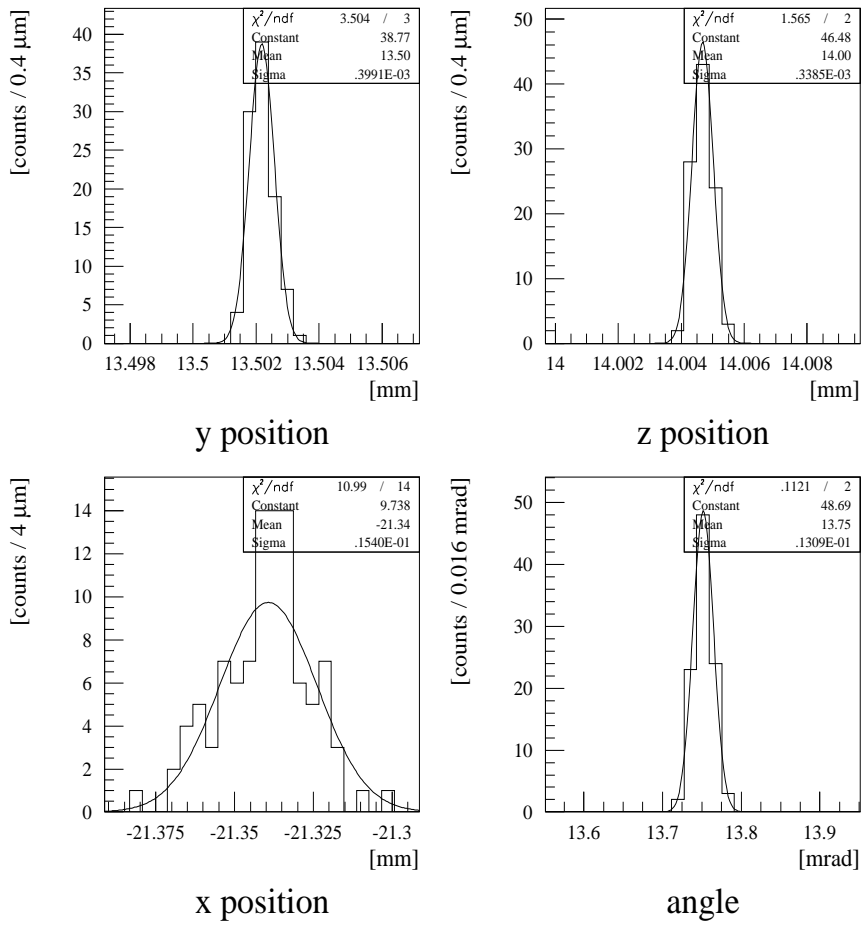


Figure 4.1 Reconstructed position and rotation angles

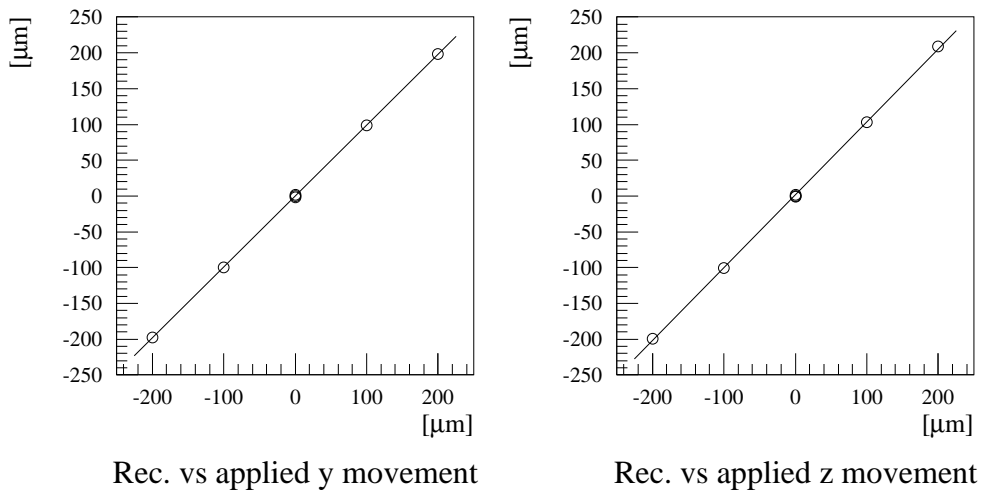


Figure 4.2 RASNIK linearity test results

Table 4.2 Comparison of RASNIK and dial gauges measurements

Displacement measured with:		
RASNIK (μm)	Gauge (μm)	Difference (μm)
52.7	47.5	+5.2
50.5	53.0	-2.5
45.7	44.5	+1.2
45.9	47.0	-1.1

5.0 RASNIK measurements and mechanical testing

After the spacer/support was glued to the first multilayer and the epoxy had cured, an initial set of RASNIK readings were made with this sub-assembly still in the jig. Assembly of the chamber was then completed as described above. A second set of RASNIK readings was then made. The difference between the two sets of data amounted to 6 μm in the y direction and 13 μm in the z direction. This was due to a combination of residual stresses in the cured epoxy and the manufacturing tolerances of the jiggling.

In July 1996, the completed BIL chamber was taken to CERN and installed in the H8 test beam area. It was suspended vertically from the support rod at the HV end of the chamber (see Section 9). RASNIK readings taken in this configuration (with no out of plane loads) showed that the chamber had a residual sag of $\sim 35 \mu\text{m}$ with respect to the zero.

Simple static load tests were done in order to compare RASNIK data with displacements measured using dial gauges and also to validate the FEA model used during design of the chamber (see ref. 6). The chamber was mounted horizontally using three support points. These mounts were not truly kinematic. A single point load of either 12 kg or 24 kg was applied at the mid point of the upper multilayer. Deflections were measured at five points along each long edge of the bottom multilayer using dial gauges with a resolution of 5 μm . RASNIK readings were taken simultaneously. The results are shown in Table 5.1. While these demonstrate generally good agreement, there are some significant differences. This can be explained by noting that the optical components of the RASNIK system are not mounted at the centre plane of the cross plates. Under load there will be some very small amount of twisting induced in the cross plates. The RASNIK system will then see an error due to the lever arm from the cross plate to the CCD and/or mask.

The same loads and mounting conditions were then used in the Ansys FEA model shown in Figure 5.1. This did not exactly model some details of the chamber construction or the mounts used at H8. In particular the dimensions of the angle brackets used to connect the cross plates to the long beams and the way in which the mounting brackets were connected to the cross plates were different. The measured sag due to the applied loads is shown in Figure 5.2 and was found to be about 20 to 25% greater than that predicted by the FEA model. Part of this difference was due to the modelling

differences noted above. Also, FEA models of this complexity are generally accurate to about 10 to 15%.

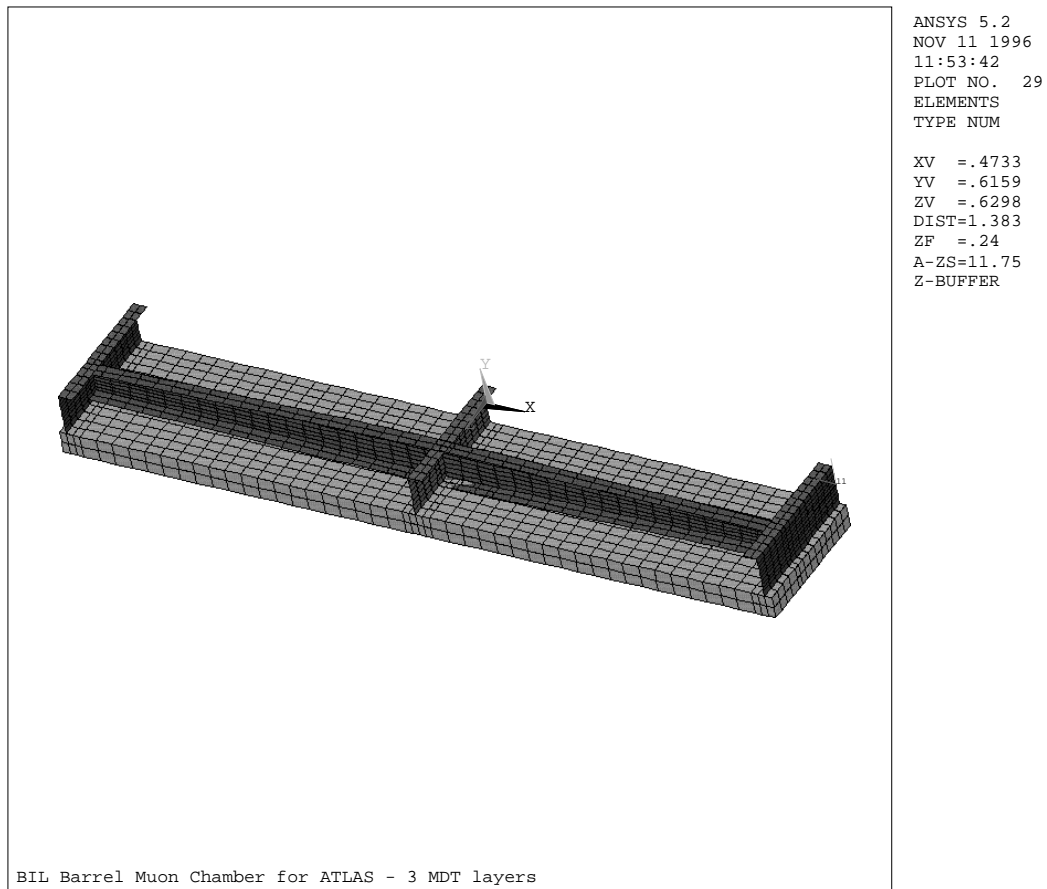


Figure 5.1 FEA model for BIL

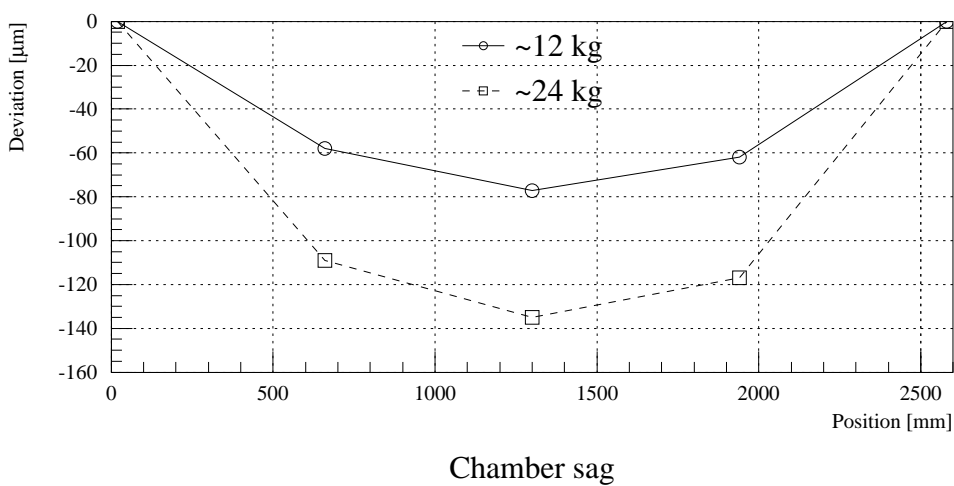


Figure 5.2 Static load deflection measurements

The BIL chamber was equipped with a pair of tension rods along each long beam and offset from the centre line of the long beam (see Figure 3.1). These are intended to

adjust the non-predictable residual sag of the chamber to zero. Tests of the rods showed that they could readily induce a controllable sag greater than any likely residual sag.

The effect of thermal gradients transverse to the multilayers was studied by using four electric blankets, each with a maximum power of 55 W. Each blanket had a ten step power regulator. In an initial pilot test, the multilayer temperatures were measured using a mercury thermometer and the chamber was heated to produce a temperature difference of up to 9°C between the multilayers. The chamber sag changed by ~150 μm. No significant heat transfer between the multilayers was seen. In a second test, a multiplexer was used to read temperature data from arrays of 24 thermistors in each multilayer. These had a precision of 0.1 °C and provided a thermal map of the chamber. The result shown in Figure 5.3 demonstrates that the chamber sag is proportional to the thermal gradient. All deformations of the chamber were found to be completely elastic for both thermal and static weight loads on the chamber.

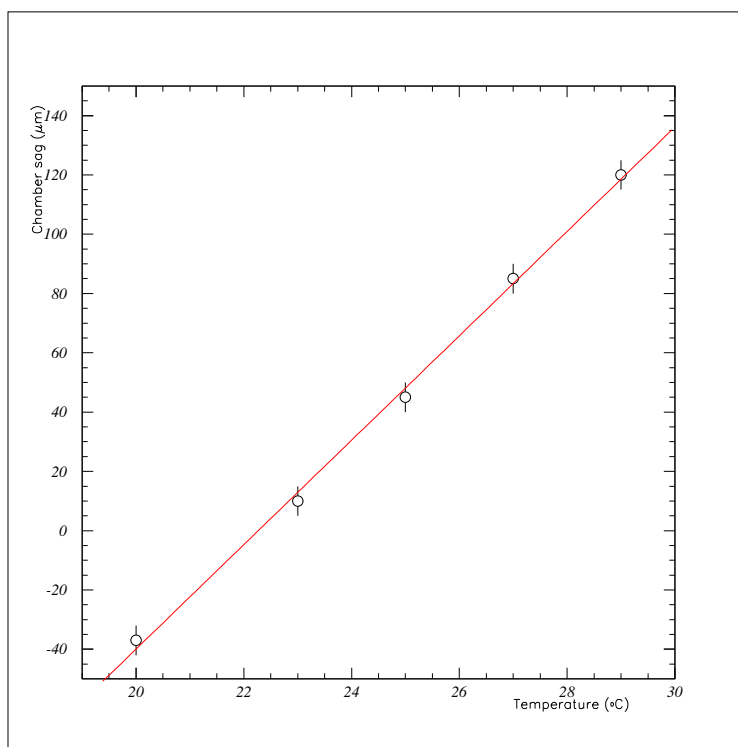


Figure 5.3 Chamber sagitta vs temperature of upper multilayer when lower multilayer is at 20°C

Table 5.1 Summary of the mechanical tests performed on the BIL prototype

Condition	Dial Gauges (μm)		RASNIK (μm)
Load ~12 kg	Right	-77	-76
Load ~24 kg	Right	-135	-148
Load ~12 kg	Left	-81	-79
Load ~24 kg	Left	-138	-153

6.0 The endplug and gas distribution system

The endplug together with its immediately associated components is one of the most critical parts of the MDT design. It has to ensure the tube gas tightness while providing reliable gas connections. It must support the anode wire under tension and, with a high degree of accuracy, centre it in the tube. It must provide reliable signal paths both to the anode and the cathode. The endplug design has not only to meet these requirements in a robust way but must do so in a manner which facilitates assembly of the tubes and of the modules.

The most important part of the endplugs employed in the construction of the BIL MDT chamber is a hollow brass pin which extends out on the axis of the tube and is threaded at its outer end. The pin fulfils many different functions simultaneously. It holds the anode wire under tension and provides the electrical connection to the wire. It provides the gas connection to the interior of the tube and a mechanical strong point which is used first to secure the gas jumpers in place and, second, to make the point of electrical connection mechanically robust. All of this is accomplished while maintaining axial symmetry. The axial symmetry makes the endplugs very simple and easy to manufacture. It also simplifies tube construction and multilayer assembly since neither the endplugs nor the tubes need to be clocked. Due to the symmetry the routing of the gas path from tube to tube is not constrained by the orientation of the tube. An exploded view of the endplug is shown in fig. 6.1.

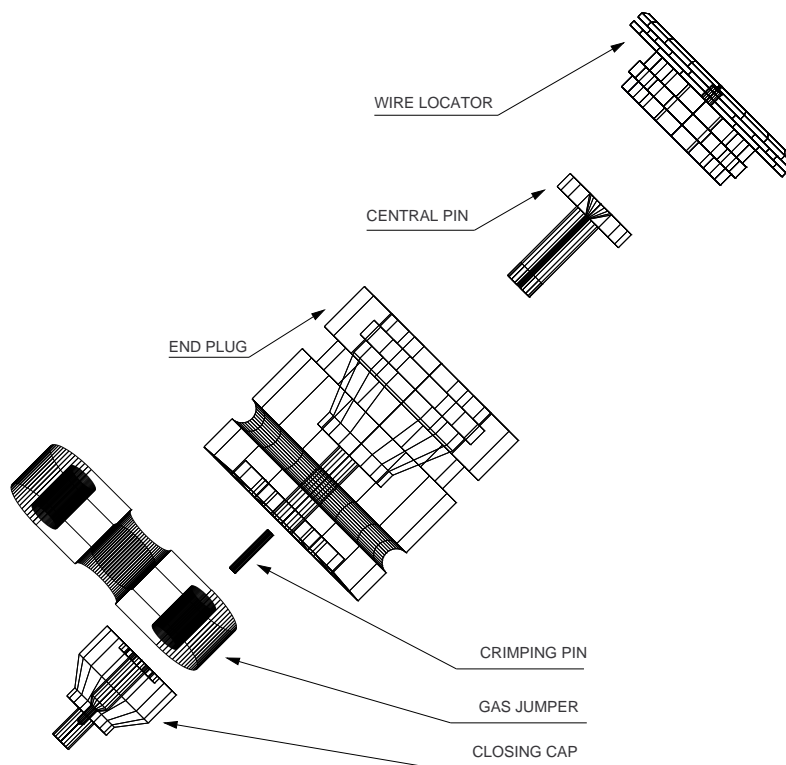


Figure 6.1 Exploded view of the endplug

The body of the plug is a cylinder made of NORYL + 30% glass (see fig. 6.2). It provides two grooves, one for electromagnetic crimping and one for the O-Ring seal

between the plug and the tube wall. The central brass pin has the function of holding

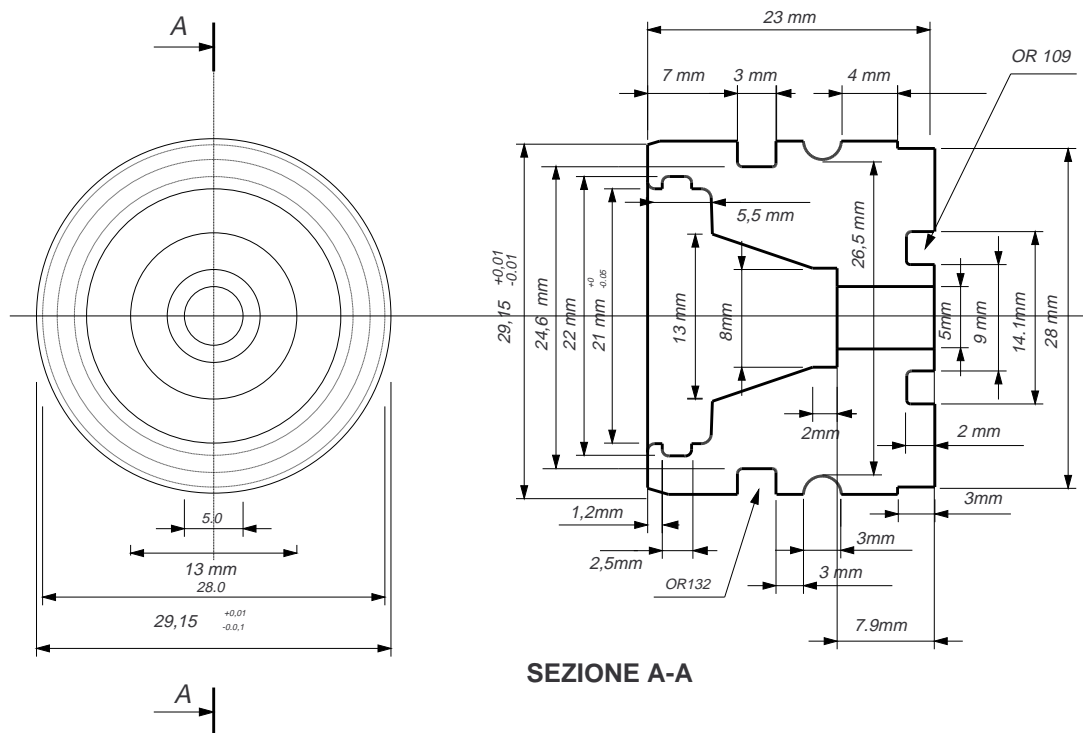


Figure 6.2 Body of the plug

the 1 mm copper tube used to crimp the wire. It has also two holes at 90° for gas circulation.

The wire locator, made of NORYL + 30% glass, consists of a disk coupled in a loose way to the plug (see fig 6.3). In this way the locator positions itself during insertion. It has a central hole drilled at high speed (60000 rpm) with a diameter of 65 μm . For the prototype the central hole was 75 μm due to the temporary unavailability of 65 μm drills and was machined and drilled on different machines with some loss of precision. This procedure was adopted for expediency.

The closing caps assure the gas tightness of the tube beyond the gas jumper and the electrical connections. On the signal side it incorporates the decoupling capacitor.

Ground pins are inserted in the empty space between the tubes and assure the ground connection both on the HV and signal sides. In this way one grounds all the tubes together, avoiding possible ground loops. For the present prototype the ground connections are made of bronze.

At present the gas jumpers have been machined using NORYL + 30% glass because the small production quantity did not justify the high cost of injection molding. Their function is to distribute the gas to neighbouring tubes (see fig. 6.4). In the BIL prototype the tubes are connected for gas distribution in groups of nine tubes in series. Each group is connected via a similar jumper to a manifold glued to the multilayer.

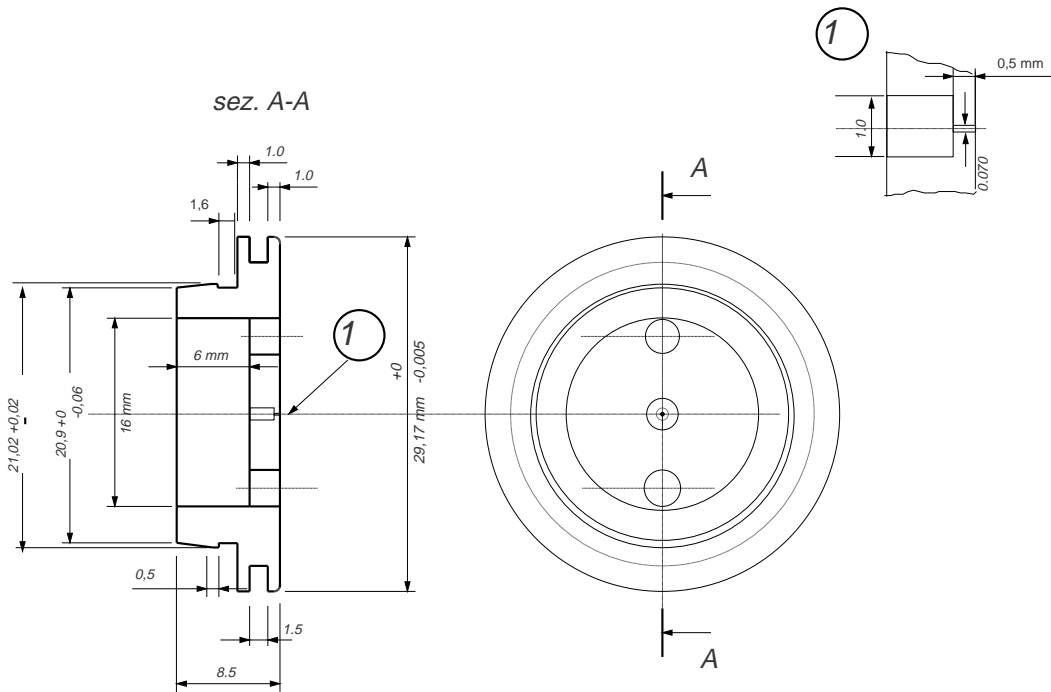


Figure 6.3 Wire locator

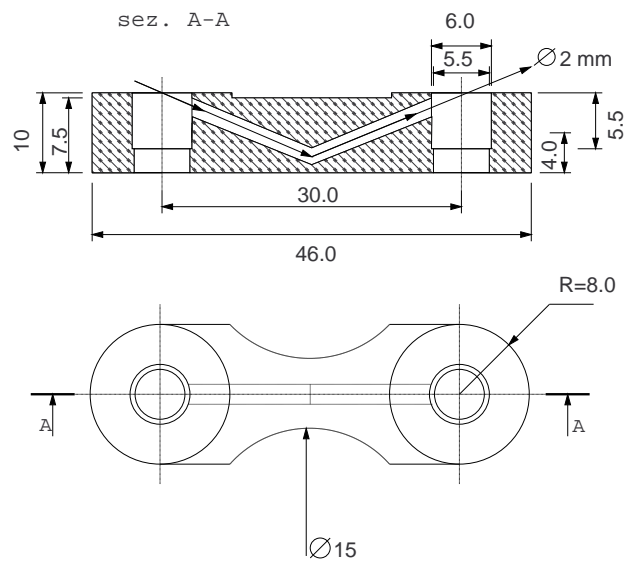


Figure 6.4 Gas jumper

7.0 Tube wiring

A prototype wiring system has been set up for wiring the tubes. It is built on a table and is partially automated. It consists of two hydraulic clamps to fix the tube on the table, two numerically controlled movements that hold the plugs and insert them into the tube, two coils for electromagnetic crimping, two hydraulic jaws to crimp the wire and an electronic tension gauge to measure the wire tension. Due to the axial symme-

try of the endplug, no specific orientation is required. The only manual operation is wire insertion into the locator, plug and pin. Based on BIL production experience, we estimate that two people are needed for tube wiring. This assumes that the tubes are already cleaned, deburred and cut to length. The average time to fabricate a tube is less than 10 minutes, which allows for a production of ~ 50 tubes/day.

The tubes were produced by METALBA, cut to length using a circular saw, deburred and cleaned using ethyl alcohol. The anode wire was 50 μm diameter W-Re produced by Luma. A total of 214 tubes was wired and tested.

The electromagnetic crimping unit was manufactured by Laboratorio Elettrofisico. It consists of a central unit providing HV supply and controls, two units containing HV capacitors (50 μF) and Hg switches and two coils. The recharging time is of the order of 5 s. The HV was set at 4.5 KV.

The wiring procedure is as follows:

- the wire is threaded into the tube;
- the tube is then positioned on the table by means of two mechanical stops and kept in position by two hydraulic clamps (see fig. 7.1);
- the wire is threaded into the wire locators and the plugs;
- the plugs are inserted into the two coils for electromagnetic crimping and kept in position by two hydraulic pistons. Each coil is fixed to a numerically controlled movement;
- the wire is threaded into the 1 mm copper tubes and then fixed at one end and attached to an electronic tension gauge on the end. The gauge is mounted on a small moving table allowing for the tensioning of the wire (see fig. 7.2);
- the two plugs are then inserted into the tubes and precisely positioned by the CNC movement in such a way that the total length of the tube, defined by the end surfaces of the plugs, is set to better than 100 μm ;
- the plug is then electromagnetically crimped to the tube (see fig. 7.3);
- the wire is tensioned to 390 g for ~ 30 seconds, then the tension is set to 350 g;
- the wire is crimped at both ends using two hydraulic jaws at a force of ~ 700 kg (see fig. 7.4);
- the finished tube is then removed from the table and sent to quality assurance tests.

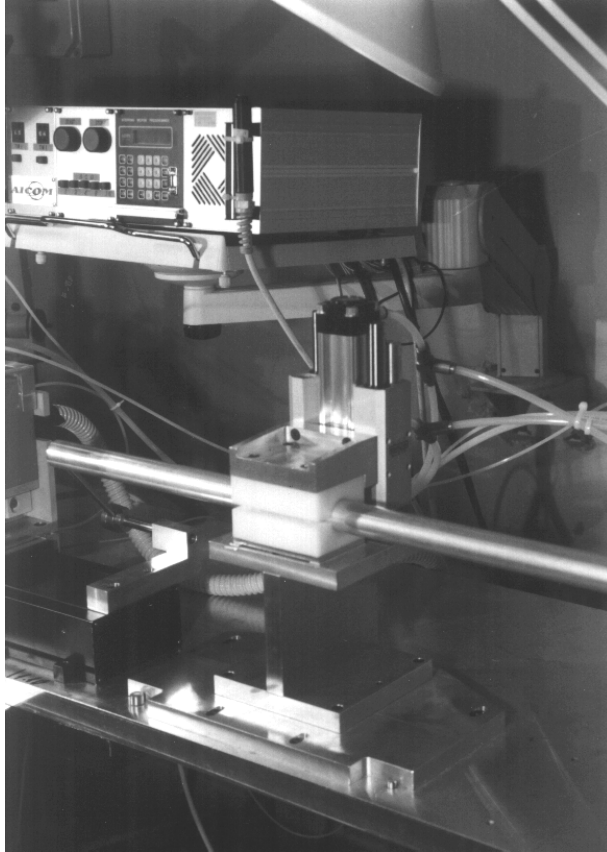


Figure 7.1 Tube clamped and positioned

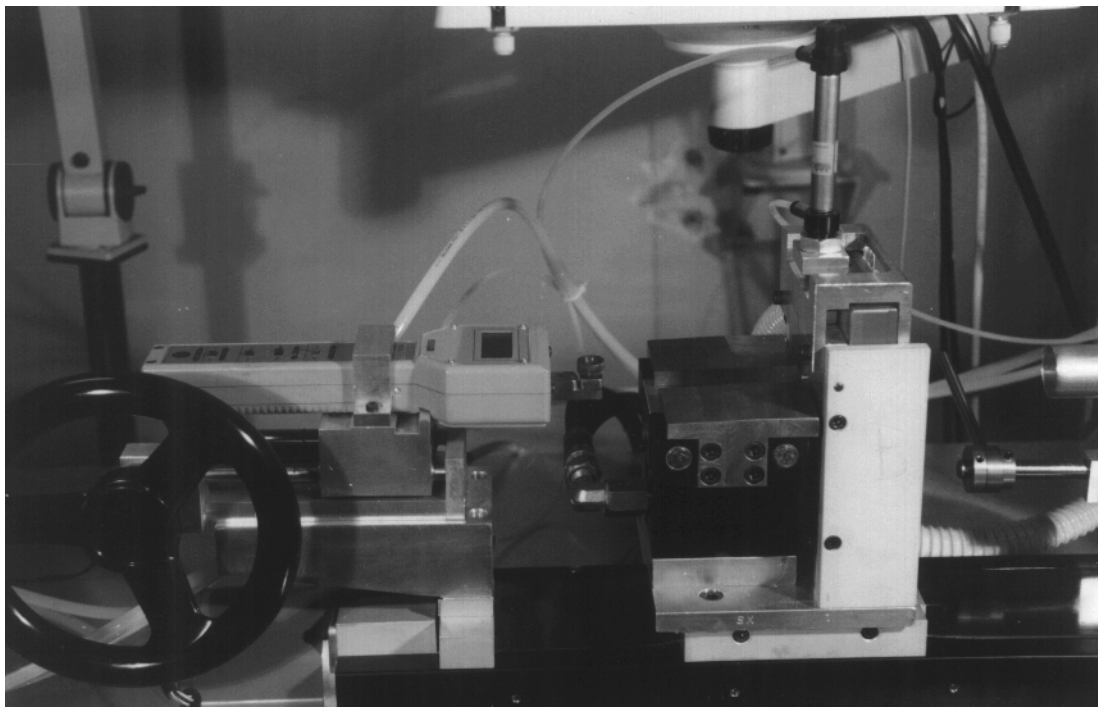


Figure 7.2 Tension gauge

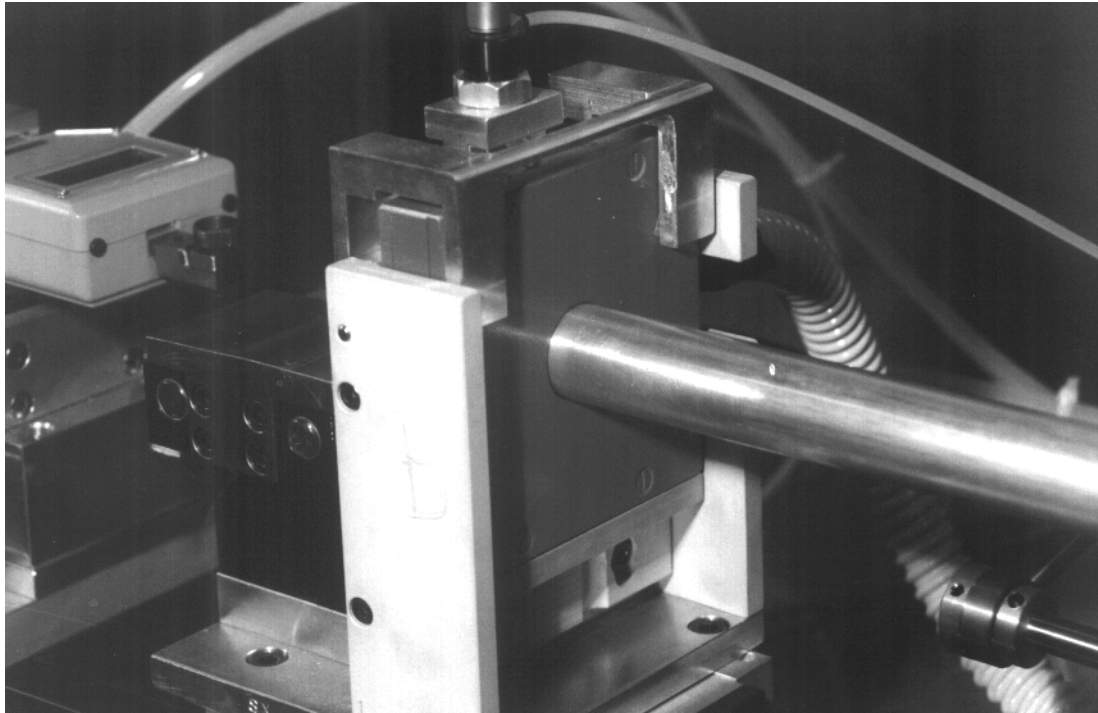


Figure 7.3 Electromagnetic crimp coil

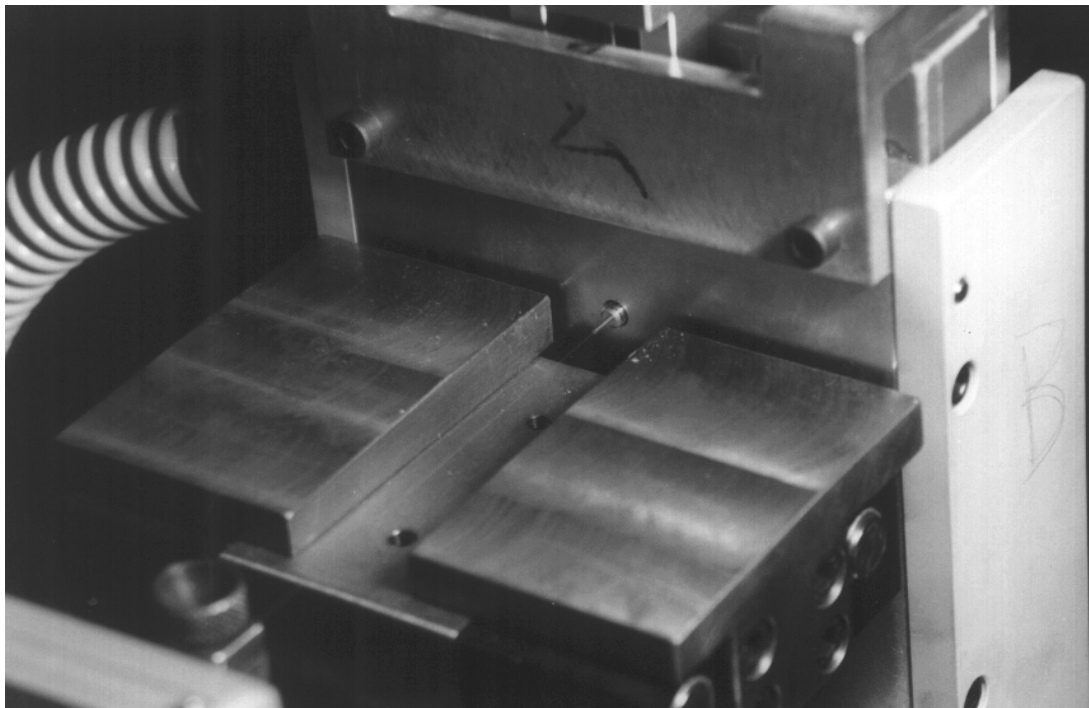


Figure 7.4 Wire crimping jaws

8.0 Quality Assurance Tests

Wire tension measurement

Wire tension was measured for all tubes with a CAEN Wire Stretch Meter unit immediately after wiring and 15 days later. The results are shown in fig. 8.1. The tension difference between the two measurements is compatible with the measurement accuracy. No tubes were rejected.

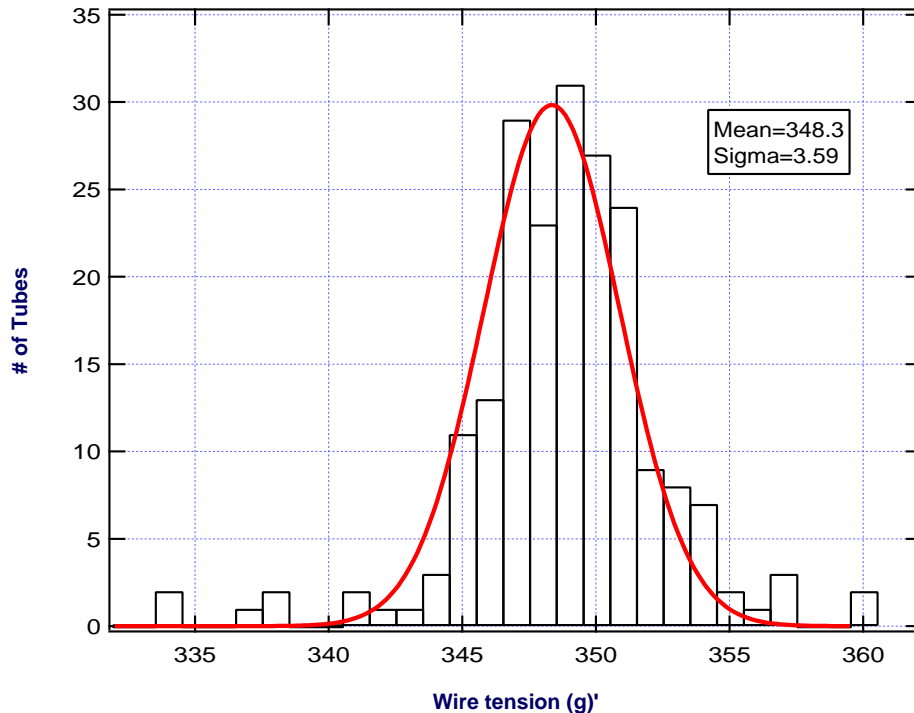


Figure 8.1 Result of wire tension measurement

High voltage tests

All tubes were high voltage tested in air. The test was performed at 3.18 KV, 150 V below the discharge limit. The current was measured using a floating nA meter. Approximately 90% of the tubes draw a current < 1 nA at the beginning and $\sim 10\%$ of the tubes had a current of 5-10 nA for a few minutes after which time the current was less than 1 nA. Two tubes had a current $> 1\mu\text{A}$ and did not recover. They were rejected.

Effectiveness of ground connections

Tests are under way exposing small modules to extreme conditions. A test module has been put in an oven in air at 50 C° for one day, at -20 C° for 1 day, in water for one day and finally in a pure oxygen atmosphere for 48 hours. Before the test the resistance between the ground pin and tube was of the order of 10-20 m Ω . After the test no sign of ground quality degradation was detected. The chamber behaviour on the test beam did not show any ground problems.

Gas tightness

All tubes were tested for gas tightness using the Brandeis method. The gas leakage was evaluated by measuring the pressure variation induced by a pump as a function of time in a small external volume connected to the tube. The sealing of the tube under test included all the components (such as O-rings, closing cap and gas jumper) foreseen for the gas distribution. The pressure was measured by an absolute capacitive manometer connected to a DVM with computer read-out. The intrinsic losses of the system were taken into account by replacing the tube with a full metal rod. The sensitivity of the measurement was 10^{-7} torr l/sec.

Fig. 8.2 shows the leak rate for the whole sample of tubes after 3 minutes of pumping, and for a sub-sample after 10 minutes. Due to outgassing, mainly caused by the

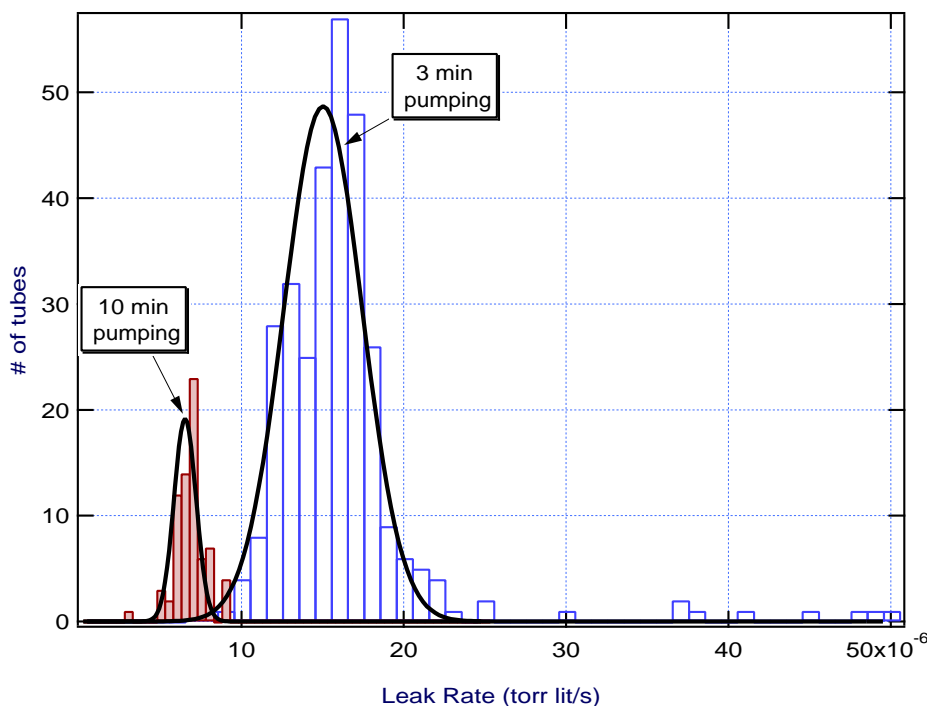


Figure 8.2 Result of leak rate measurement

plastic components of the end-plug, the leak rate was observed to decrease with time during the initial pumping phase, a stable condition being reached after a few hours. No tube showed a leak larger than 10^{-5} torr l/sec.

The maximum leak rate allowed for operation in the experiment is 10^{-5} torr l/sec for a single tube. Such a limit is already approached after 3 minutes of pumping. Extrapolating we conclude that for all the tubes in the sample the leak rate is about an order of magnitude lower than the requested limit.

A leak test on the complete chamber was also done at 3 bar at CERN at the end of the test beam period and resulted in a leak rate of 0.15 bar l/h.

Gas contamination

Preliminary analysis with a mass spectrometer of the outgassing products from NORYL has been performed. The measurement shows traces of water, nitrogen and oxygen and no gases known to contribute to ageing.

9.0 Read-out Electronics and HV

The read-out chain used for the BIL prototype consists of four stages: preamplifier, shaping amplifier, discriminator and TDC. The preamplifier, shaping amplifier and discriminator designed at Brookhaven National Laboratory [7] are each realized in thick-film hybrid technology with a single channel per chip.

The preamplifier has a bipolar transistor input in a common-base configuration which is followed by two emitter follower stages. The input impedance is approximately 87Ω and the single-ended output is capable of driving long 50Ω coaxial cables which connect the preamplifier output to the input of the shaping amplifier.

The preamplifiers are mounted on a hedgehog board (the lower board in fig. 9.1). With no tubes connected the measured cross-talk of the preamplifier boards is of the order of 0.1%. Each board houses 24 amplifiers and each amplifier connects directly to the bonnets of the HV decoupling capacitors. A total of 8 boards is required for the BIL chamber.

The shaping amplifier consists of three active stages which are coupled together by two pole-zero networks for tail cancellation. It has the same basic configuration of the preamplifier. The single-ended output is set to give a pseudo-gaussian signal with 12 ns peaking time.

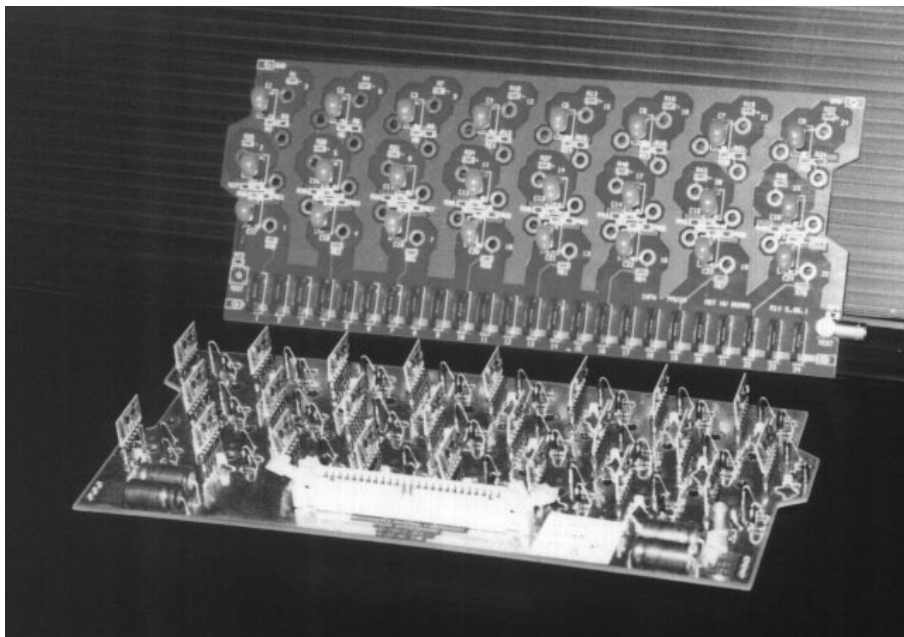


Figure 9.1 Hedgehog preamplifier board (lower) and high voltage board (upper)

The shaping amplifiers are mounted on a board which has the same dimensions as a Fastbus board but does not contain the segment and auxiliary connectors. They are mounted in a Fastbus crate but voltage is supplied through an AMP Mate-N-Lock connector. Each board contains 48 shaping amplifiers.

The preamplifier and shaping amplifier are AC coupled. Each preamplifier board is connected by a 10 m long, 24 channel coaxial flat cable. The combined gain of the preamplifier and shaping amplifier is in the range 15 to 25 mV/fC. For the test data discussed in section 10.0 we operated with a gain of approximately 15 mV/fC. The equivalent noise charge with no input capacitance is of the order 103 electrons.

The discriminators are ECL comparators with differential outputs. They are mounted in units of 48 on a Fastbus-like board which is mechanically identical to the shaping amplifier boards. This board receives signals from the shaper board via 0.5 m long coaxial flat cable. The 25th electron (primary ionization) corresponds to a threshold of 770 mV.

The discriminator outputs were connected by 25 m twisted pair cables to TDC's in the counting room. For the test beam data half the chamber was read out by KEK TDC's which have 0.78 ns time resolution and the other half with KLOE TDC's which have 1 ns time resolution.

High voltage is supplied to the tubes at the end opposite to the preamplifier connection. Each tube has a 1 M Ω series resistor and 1 nF filter capacitor and is terminated on this end by a 390 Ω resistor. These passive components are mounted on printed circuit boards, the upper board in fig. 9.1, that are like the preamplifier boards.

The rate of spurious TDC hits measured with high voltage cables disconnected is less than 0.1% for all channels. There is no increase in the spurious hits when connections to the HV supplies are properly filtered and terminated.

In the test beam we observed that the 48 temperature probes in the interstitial spaces between the tubes were a source of noise for the tubes nearest to the probes. In the production chambers the few temperature sensors will all be on the surface of the multilayer and not embedded in the multilayer so this will not be a problem.

10.0 Test beam results

The BIL prototype has been extensively tested on the CERN H8 beam during summer 1996. The chamber was installed with the tubes in vertical position (in order to eliminate the gravitational sag of the wire) and perpendicular to the beam axis. The 10 * 10 cm² trigger covered an area near the centre of the chamber and the beam intensity was usually kept below 20 Hz/cm² to avoid possible space charge problems. The chamber was operated in proportional mode at 3.25 KV (corresponding to a 2*10⁴ gain) with Ar (91%), N₂ (4%), CH₄ (5%) mixture¹, and with a threshold setting on the 25th electron. The read-out chain is the one described in section 9. HV, threshold and beam intensity scans around the operating conditions were also performed.

1. This mixture is the present baseline option for the MDT operation [8].

The analysis of the data is in progress and will be presented in a separate Muon Note. Here we present only preliminary results on the single tube resolution in the reference operating conditions.

A typical time spectrum of a tube is shown in fig. 10.1; the few per cent noise level visible in the figure was easily removed by asking for a time coincidence with the corresponding tubes in the same multilayer.

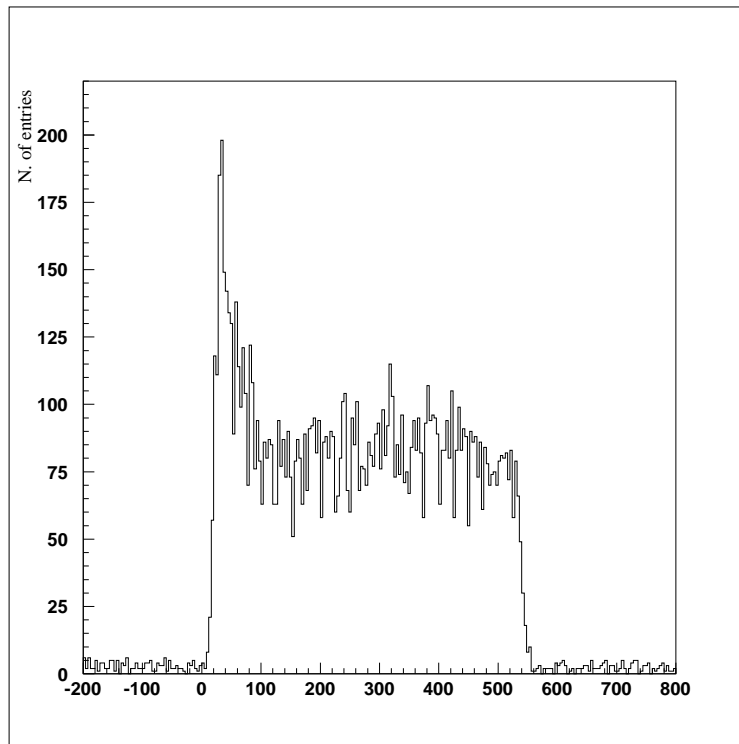


Figure 10.1 Typical time spectrum of a tube

The standard autocalibration procedure described in ref. [9] was used for the r-t relation optimization. The individual channels t_0 's were obtained by fitting a Fermi-Dirac function to the rising part of the time spectrum (see fig. 10.2) plus a fine adjustment based on track fit residuals. The accuracy obtained by this procedure has been measured to be < 0.7 ns.

For autocalibration the nominal wire position was assumed and the same r-t relation was used for all the tubes illuminated by the beam. Autocalibration procedure was applied to each multilayer separately and then the two r-t relations compared. Differences were all less than $50 \mu\text{m}$. The single wire resolution, as a function of the radial distance from the wire, was obtained by fitting a straight line using 5 out of 6 tubes of the two multilayers and calculating the residuals of the 6th.¹ The result for a typical tube is shown in fig. 10.3. A resolution of $\sim 80 \mu\text{m}$ for $r > 0.3$ cm is observed and the average over all the radii is around $95 \mu\text{m}$. The continuous lines are the predictions from the Garfield-Magbolz simulation [10] for the total resolution and for the

1. In the fit the error dependence from the radial position of the hit was used. The procedure was iterative; in the first step constant errors were used and the resolution dependence on r was measured on the 6th tube. This resolution was then re-injected in the fit and the final resolution vs r was obtained.

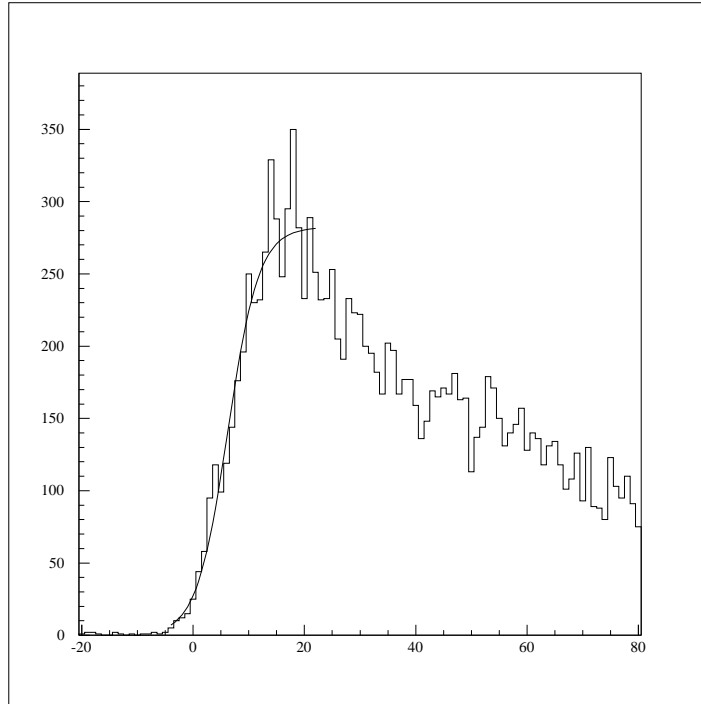


Figure 10.2 Rising edge of the time spectrum and the fitted Fermi-Dirac function

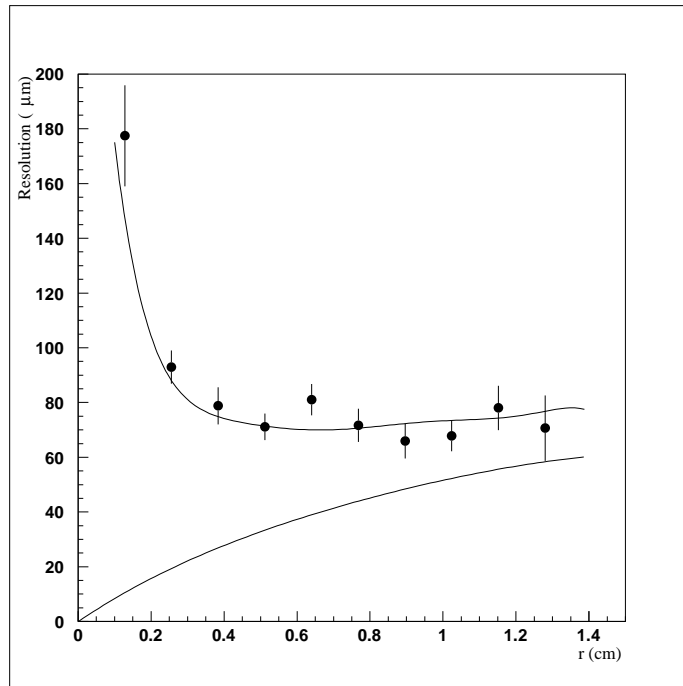


Figure 10.3 Resolution vs radial position of the track

diffusion contribution only. There is remarkable agreement between the data and the Garfield-Magbolz prediction.

Figs. 10.4 and 10.5 show respectively the angular and intercept difference, in the chamber middle plane, obtained from the fits of the same track in the two individual

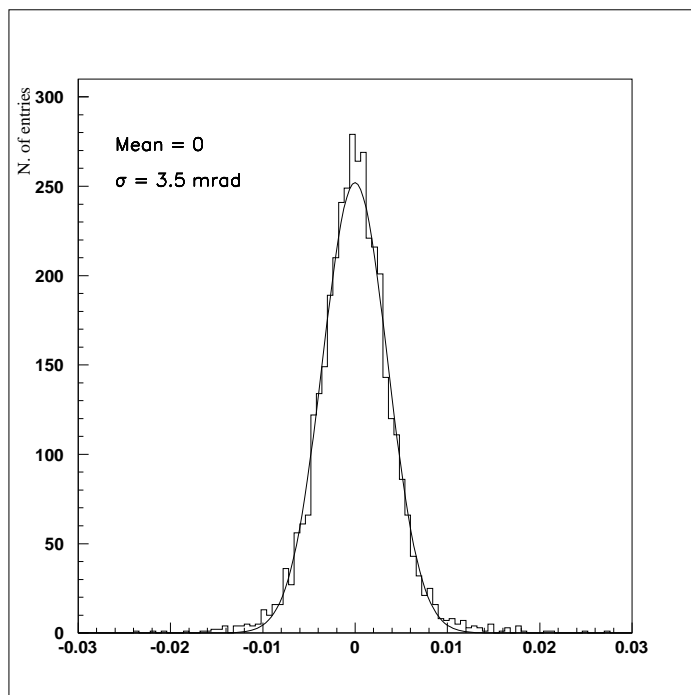


Figure 10.4 Angular difference between the two straight lines obtained by fitting hits on each multilayer

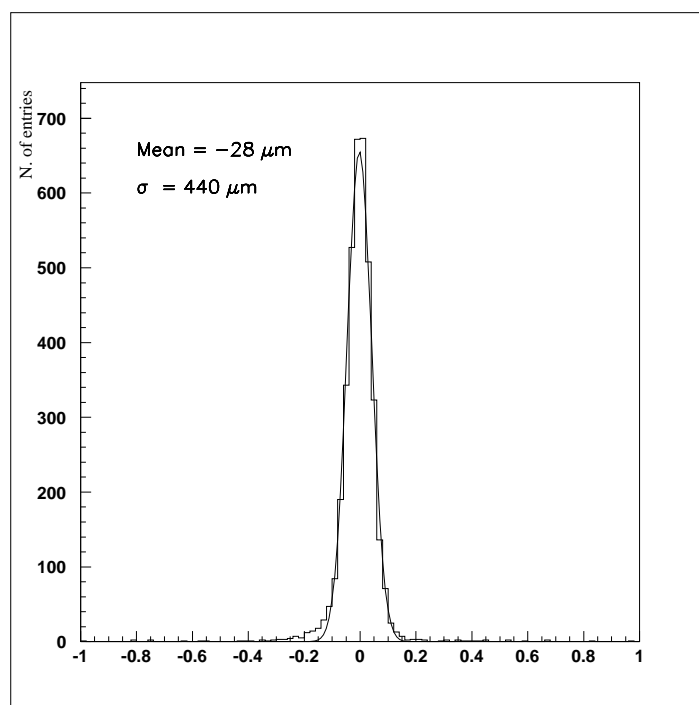


Figure 10.5 Position difference, at the chamber middle plane, obtained by fitting hits in each multilayer

multilayers. The systematic shift in angle is less than $10 \mu\text{rad}$ and the relative displacement is of the order of $30 \mu\text{m}$.

11.0 Conclusions

A first full scale prototype of an MDT-BIL chamber has been built using the jiggling approach proposed from Seattle and a simplified spacer/support structure based on the one developed for the end cap MDT chambers.

A rotational invariant endplug/wire locator prototype, satisfying the electrical and gas tightness specifications, has been developed and used for the tube construction.

A semi-automatic wiring table has been built and tested in the tube fabrication; typical wiring speed was ~ 50 tubes/day.

The in-plane alignment system has been installed and successfully tested. The measured mechanical properties of the chamber show reasonable agreement with the FEA predictions.

Thermal tests have measured the expected chamber deformation under thermal gradients between multilayers.

The first results from the test beam indicate a single-wire resolution of $\sim 80 \mu\text{m}$ in excellent agreement with the Garfield-Magbolz simulation. The good results from the autocalibration and from the matching between the two multilayers, obtained with nominal wire positions, indicate, at least locally, a relative wire positioning within specifications.

References

- [1] ATLAS Technical Proposal. CERN/LHCC/94-43
- [2] C. Daly et al. - Concept for the Design and Assembly of Forward Region MDT Chambers for ATLAS. - ATLAS Muon Note-086
- [3] L. He et al. - A simple method for precise alignment of mechanical elements over very large distances. - ATLAS Muon Note to be published
- [4] H. Guldenmann et al. - On Gluing Tubes into Multilayers. - ATLAS Muon Note-118
- [5] The ATLAS Muon Group - The alignment of the ATLAS Muon Spectrometer - ATLAS Muon Note-113
- [6] C. Daly et al. - FEA Analysis of a Large MO Muon Chamber for ATLAS. - ATLAS Muon Note 048/95.
- [7] J. Fischer et al., Nucl. Inst. and Meth. A238, 249-264 (1985).
- [8] The ATLAS Muon Detector Physics Group - Criteria for the Choice of the MDT Operating Point - ATLAS Muon Note-098
- [9] C. Bacci et al. - Autocalibration of high precision drift tubes. - ATLAS Muon Note-135
- [10] W.Riegler, private communication.